AGU PUBLICATIONS

JGR

Journal of Geophysical Research: Atmospheres

RESEARCH ARTICLE
10.1002/2013JD020499

Key Points:
- First 10 year observations of gravity waves in Africa
- Contribution of thunderstorms in the production of gravity waves
- Climatology of gravity waves from thunderstorms in Africa

Correspondence to:
E. Blanc,
elisabeth.blanc@cea.fr

Citation:
Blanc, E., T. Farges, A. Le Pichon, and P. Heinrich (2014), Ten year observations of gravity waves from thunderstorms in western Africa, *J. Geophys. Res. Atmos.*, *119*, 6409–6418, doi:10.1002/2013JD020499.

Received 4 JUL 2013
Accepted 28 APR 2014
Accepted article online 3 MAY 2014
Published online 10 JUN 2014

Ten year observations of gravity waves from thunderstorms in western Africa

E. Blanc[1], T. Farges[1], A. Le Pichon[1], and P. Heinrich[1]

[1]CEA DAM DIF, Arpajon, France

Abstract A new study of gravity waves produced by thunderstorms was performed using continuous recordings at the IS17 (Ivory Coast) infrasound station of the International Monitoring System developed for the verification of the Comprehensive Nuclear Test-Ban Treaty. A typical case study is presented for a large thunderstorm on 10–11 April 2006 lasting near 14 h. Comparison with cloud temperature measured by the Meteosat 6 satellite shows that wave activity is large when the cloud temperature is low inside convection cells located over the station. Statistics based on 10 year data show that the wave activity is intense throughout the year with peak periods in May and October and less intense activity in January, in good agreement with the local keraunic level. The seasonal variations of the wave azimuth highlight clear trends from northward direction from February to August to southward direction from August to December. Lightning flashes, observed from space, show a similar motion confirming that thunderstorms are the main sources of the gravity wave activity. The gravity wave azimuth follows the seasonal motion of the tropical rain belt partly related to the Intertropical Convergence Zone of the winds. The contribution of other possible sources, such as wind over relief, is weak because surface winds are weak in this region and only oceans are present south of the station. We conclude that the large observed wave activity is mainly produced by convection associated to thunderstorms.

1. Introduction

Thunderstorms are an efficient source of atmospheric waves. Infrasonic waves at periods 20–50 s produced by thunderstorms were tracked by microphone arrays in the 1960s [*Goerke and Woodward*, 1966]. Such waves were associated to the leading edge of the storms. At larger periods from 10 to 20 min, gravity waves characterized by frequencies lower than the Brunt Väisälä period were also observed by microbarometers up to distances of hundreds of kilometers from thunderstorm regions in relation with convection [*Curry and Murty*, 1974]. *Gratchev et al.* [1988] measured waves at periods ranging from 20 to 180 min when thunderstorms passed over the station. The different wave oscillations were related to several convective cells within the thunderstorm [*Grachev et al.*, 1995].

New interest in the atmospheric waves produced by thunderstorms arose with the sprite discovery [*Sentman and Wescott*, 1993] and related observation campaigns using complementary instrumentation [*Lyons et al.*, 2008; *Neubert et al.*, 2008; *São Sabbas et al.*, 2010]. Sprites are transient luminous events generally observed by cameras at the horizon, but they also generate infrasound [*Liszka*, 2004; *Farges et al.*, 2005]. However, the sprite energy is not sufficient to generate larger-scale waves which could be detected in the mesospheric OH airglow layer. Only concentrically expanding gravity wave ripples generated by the thunderstorm convection circular structure were observed in the mesosphere [*Sentman et al.*, 2003]. *Pasko et al.* [1997] showed that gravity waves launched by thunderstorms could lead to vertically oriented cylindrical structures in the mesosphere above the thunderstorm closely resembling to some sprite structures. Also, a clear correlation was observed between acoustic gravity waves and the sprites, the tops of sprites appearing to align with the acoustic gravity wave depletions in the 80 to 95 km altitude region [*Siefring et al.*, 2010].

The development of the International Monitoring System (IMS) infrasound network dedicated to the verification of the Comprehensive Nuclear Test-Ban Treaty (CTBT) motivates new scientific studies. This network will consist of 60 infrasound stations distributed uniformly over the surface of the globe [*Christie and Campus*, 2010]. The microbarometers used at each station provide high-quality data, and correlation-based processing techniques determine the wave front parameters (e.g., direction of arrival and horizontal phase velocity). Infrasound inversion methods were developed. Such processing allows, for example, to determine the infrasound origin of sprites at altitudes from 40 to 100 km [*Farges and Blanc*, 2010].

As most microbarometers are characterized by a broad bandwidth, larger-scale atmospheric waves like gravity waves and tides can also be observed [*Marty et al*., 2010]. Gravity waves modulate the wind profiles, producing partial reflections of infrasound in the stratosphere and strong modifications of the detected infrasound waveforms [*Kulichkov and Bush*, 2001]. The most recent infrasound attenuation relations incorporating such effects are used to predict the network detection capability in time-varying and range-dependent conditions [*Le Pichon et al*., 2012].

Observations of gravity waves are of large interest for scientific applications and operational monitoring. However, the wave characteristics and associated source mechanisms need to be better understood. The present study aims to quantify the gravity wave activity in West Africa equatorial region where thunderstorms are very intense [*Christian et al*., 2003]. Early gravity wave observations in the equatorial ionosphere showed large gravity waves at periods of 5–30 min originating from the rain forest where convection takes place [*Rottger*, 1977]. This suggests that convection could be at the origin of strong gravity wave activity penetrating in the upper atmosphere and ionosphere with a possible impact on the general atmospheric circulation. This was confirmed by equatorial observations in the mesospheric airglow layer in Indonesia showing that gravity waves are directly related to the horizontal distribution of wave sources such as cumulous clouds near the observation site [*Nakamura et al*., 2003]. For waves at low and middle latitudes, their upward propagation to the mesosphere may be significantly influenced by wave filtering or ducting by stratospheric winds [*Medeiros et al*., 2003; *Pautet et al*., 2005].

The gravity waves produced by thunderstorms can propagate vertically into the stratosphere, mesosphere, and lower thermosphere and, by mechanical forcing, can excite secondary short-period waves, which can be trapped in the lower thermosphere and propagate over large distances [*Vadas et al*., 2003; *Snively and Pasko*, 2003]. Near their sources, they form concentric rings in the mesosphere as observed by all-sky airglow layer imagers [*Alexander et al*., 2004; *Yue et al*., 2009]. The cumulative effects of gravity wave activity could then constitute an important large-scale wave source which may disturb the general atmospheric circulation [*Holton et al*., 1995; *Baldwin et al*., 2003; *Shaw and Shepherd*, 2008]. A strong air descent observed by satellite in northern polar regions by *Hauchecorne et al*. [2007] was explained by a pure atmospheric dynamical phenomenon induced by gravity wave activity. For improving modeling of the middle atmosphere dynamics and weather forecasting [*Charlton et al*., 2004; *Lott and Guez*, 2013; *Mitchell et al*., 2013], the occurrence, amplitude, and impact of gravity waves need to be determined. The contribution of waves originating from thunderstorms and convection compared to other orographic sources needs also to be quantified.

We consider here 10 years of gravity wave observations performed at the IS17 (Ivory Coast 6.67°N, 4.85°W) IMS station located within the ITCZ (Intertropical Convergence Zone), together with lightning and cloud temperature measurements. The use of IMS data in this low-frequency range is very recent. Such new observations can provide a realistic representation of the gravity wave spectrum in the troposphere and open new scientific objectives.

After a presentation of infrasound technology and data processing, we describe wave activity during a large typical thunderstorm and show the formation of intense gravity waves in convection cells corresponding to low-temperature clouds. We then analyze the climatology of the gravity wave activity and demonstrate that most of this activity is produced by thunderstorms. In the framework of the Atmospheric Dynamics Research Infrastructure in Europe (ARISE; http://arise-project.eu) project, we discuss the influence of gravity waves produced by thunderstorms at low latitude on the global dynamics of the Earth's atmosphere and their possible impact on weather and climate.

2. Observations

2.1. Methodology

The infrasound network developed for the verification of the CTBT will include 60 stations uniformly distributed across the globe when it will be completed. The first infrasound station was certified in 2001. Today, nearly 70% of this network is operational. The IMS network is unique by its global and homogeneous coverage as well as its data quality. It is larger and much more sensitive than any previously operated infrasound network. All technical aspects of infrasound monitoring related to sensors, stations, and data processing have been redeveloped for CTBT verification [*Christie and Campus*, 2010; *Brachet et al*., 2010].

Stations are very sensitive acoustic antenna including at least four microbarometers at distances of 1 to 3 km, with a flat frequency response between 0.01 and 8 Hz, a sensitivity of about 0.1 m Pa, and a large dynamic scale of 80 dB [*Ponceau and Bosca*, 2010]. These arrays are able to detect and characterize low-amplitude coherent infrasound signals within the background noise. In order to improve the signal-to-noise ratio (by ~20 dB), infrasound arrays are connected to optimized wind noise reduction devices [*Ponceau and Bosca*, 2010]. The large dynamics of the instruments allow the observations of large-amplitude events close to the station and small-amplitude signals from remote sources. Recent technical advances in the development of efficient algorithms allow detecting coherent waves within noncoherent noise. The Progressive Multichannel Correlation (PMCC) method is routinely used to characterize low-amplitude pressure signals in real time [*Cansi*, 1995]. Using such an approach, different coherent wave systems can be differentiated by their time-frequency signature and azimuth.

In the last decade, detection bulletins determined from near-real-time analysis were produced and correlated with observations of natural or man-made atmospheric sources, such as exploding meteoroids, volcanic eruptions, hurricanes, earthquakes, and ocean swelling [*Campus and Christie*, 2010; *Le Pichon et al*., 2013; *Matoza et al*., 2013]. More recently, well-determined repetitive infrasound sources are used to probe the upper atmosphere [*Le Pichon et al*., 2005; *Lalande et al*., 2012; *Assink et al*., 2012]. Gravity waves and tides can be observed with most of the microbarometers in the lower frequency range of the instrument below the Brunt Väisälä frequency. This frequency range is lower than the one generally used for infrasound observations (0.02–4 Hz). However, the high quality of the low-frequency observations was demonstrated using specific validation experiments [*Marty et al*., 2010] and analysis of some large-scale disturbances including tides, solar eclipses, and large-scale waves from thunderstorms [*Blanc et al*., 2010; *Marty et al*., 2013].

2.2. Data Processing

The IS17 Ivory Coast station is composed of four MB2000 microbarometers forming a triangle of ~ 1km basis with a central point which is a typical configuration of IMS stations [*Christie and Campus*, 2010]. Such stations form sensitive acoustical antennas. The PMCC data processing algorithm is based on a progressive study of the correlation functions leading to a consistent set of time delays in the case of a coherent propagating wave. Detection is determined on the basis of signal consistency. In case of detection the time delays are used to compute the signal azimuth and phase velocity [*Cansi*, 1995]. This array processing method was originally designed for seismic data and proved to be efficient for extracting low-amplitude coherent infrasound signals among noncoherent noise [*Le Pichon and Cansi*, 2003]. It is then intensively used for operational processing for detection of events and a tool to analyze the signals detected by the IMS stations. Different wave systems are routinely differentiated from their wave signature in time and frequency and from their wave azimuth and phase velocity. The processing is performed in different frequency bands between 0.07 and 4.0 Hz and in adjacent time windows covering the whole period of analysis. Detections characterized by similar characteristics can be grouped in detection clusters forming events. Additional details are given by *Brachet et al*. [2010]. The method is very sensitive and allows representation of persistent oscillations by a sequence of similar events if small changes in azimuth and velocity are identified.

In the present paper, the analysis has been adapted to larger time periods for gravity wave studies. The capability of the sensors for such observations was validated by *Marty et al*. [2010]. As the sensor low cutoff frequency is set at 9.8 10^{-3} Hz, the entire gravity wave frequency range is attenuated by the filter. The maximum error due to the filtering uncertainties was determined using data from field experiments. The error was found at least 34 dB lower than the noise power spectral density, demonstrating that the IMS pressure measurements can be accurately corrected a posteriori from filtering effects [*Marty*, 2010]. This led to first studies at low frequency using this technology, including analysis of gravity waves [*Blanc et al*., 2010] and larger-scale ground pressure fluctuations produced by the passage of solar eclipses [*Marty et al*., 2013].

Figure 1 presents an example of the PMCC analysis performed for a large thunderstorm on 10–11 April 2006 measured in the I17 IMS Ivory Coast station. The signals recorded by the four different sensors in the 0.001 to 0.0001 Hz frequency range present a good coherency, and the correlation coefficient is close to unity. Figures 1b and 1c display, in time-frequency diagrams, the wave azimuth and phase velocity in color, respectively. We then explain the observations as produced by the gravity waves at their origin, inside, or very near the convection cells. Figure 1 shows that the azimuth follows the thunderstorm motion. The velocity does not significantly change during the event. This differs from other observations of faster gravity waves before the passage of convective cells reported, for example, by *Danilov and Svertilov* [1991].

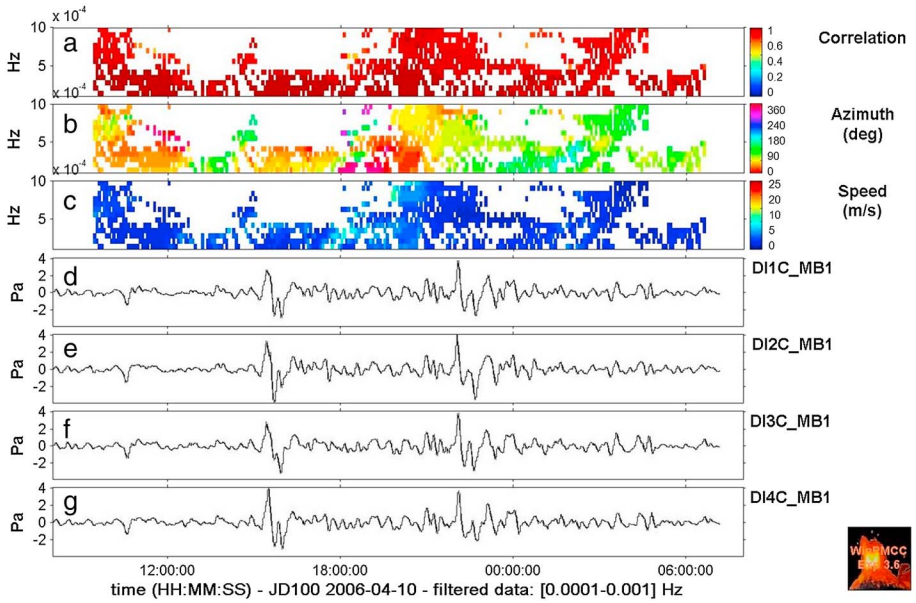

Figure 1. Example PMCC data processing using data recorded at the IS17 IMS station during the thunderstorm of 10–11 April 2006. The data processing was performed in the gravity wave frequency range. The figure displays (d–g) the time series of the four station components, (a) the correlation coefficient, (b) the azimuth, and (c) phase velocity.

The corresponding wavelet data processing (Figure 2) shows that the signal frequency varies from 8 min to few hours. Tides are observed at 12 and 24 h in the lower frequency part of the signal, showing the sensor capability to perform observations at low frequencies.

2.3. Wave Activity During the Thunderstorm of 10–11 April 2006

The meteorological conditions corresponding to this same thunderstorm are given by the radiance temperature maps measured at the cloud top by the Meteosat 6 satellite and shown in Figure 3. A general westward motion of the clouds can be observed during the thunderstorm duration.

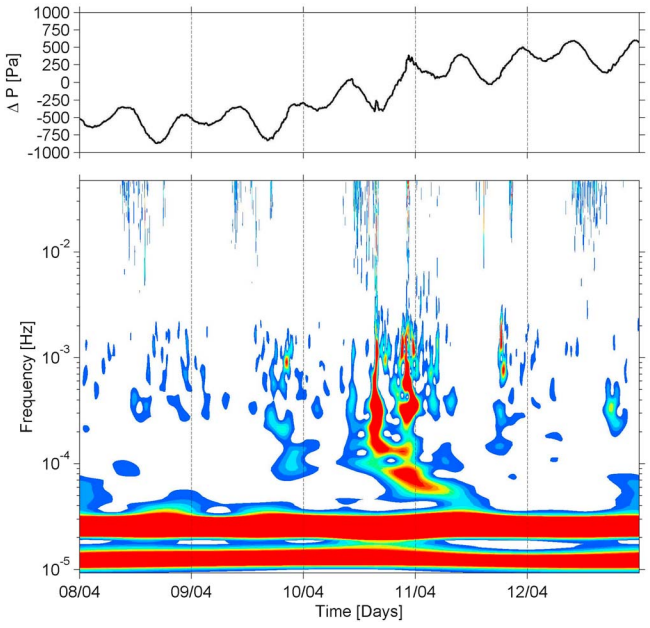

Figure 2. Wavelet analysis for the same thunderstorm. The upper part of the figure shows the absolute pressure measured by one of the station sensor.

A first gravity wave maximum is observed between 15:00 and 16:00 UT while a cloud cell appears just over the station. The wave azimuth is about 60°. It roughly corresponds to the general southeastward thunderstorm motion. The wave period is about 1 h, and the wave amplitude reaches 5 Pa peak to peak (~160 Pa after correction of the microbarometer frequency response). The second maximum, between 21:30 and 23:00, corresponds to the passage of a second thunderstorm cell. It is correlated with a low temperature (−80°C) of the cloud above the station indicating an area of strong convection [*São Sabbas et al.*, 2010]. The different azimuths identified between 00:00 and 03:00 UT indicate a multicellular structure of the storm, suggesting the possibility to determine the origin of the gravity waves inside the convection

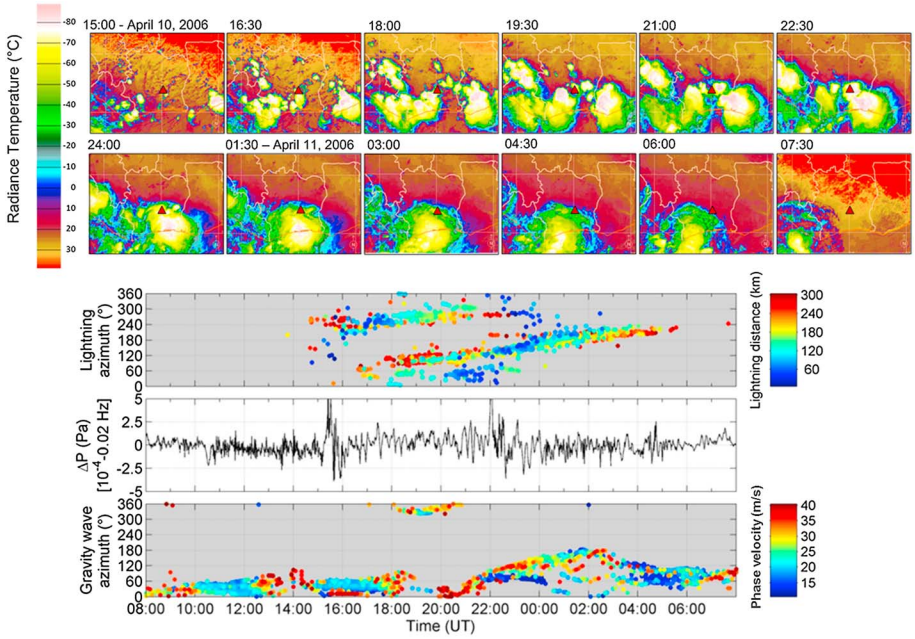

Figure 3. (top) Meteosat 6 maps of the radiance temperature at the top of the thunderstorm clouds for the same thunderstorm. The station location is indicated by the red triangles. The thunderstorms are moving westward. (bottom) The increase of the gravity wave amplitude corresponds to the passage of the thunderstorm convective cells close to the station. The azimuth roughly corresponds to the thunderstorm azimuth. At 22:00 UT, several directions are distinguished, indicating a multicellular structure.

cells, as it has been recently demonstrated by *Costantino and Heinrich* [2013]. The lightning activity observed by the Worldwide Lightning Location Network (WWLLN) [*Rodger et al*., 2009] starts at 15:00 when the cloud appeared over the station (Figure 1b). The lightning azimuths were computed assuming observations from the station. The lightning distance to the station is represented by the color. The lightning azimuth at distances lower than 120 km (in blue) differs from the gravity wave azimuth. The thunderstorm mechanisms for producing gravity waves are not related to lightning activity but rather to the convection cells moving over the station.

2.4. Seasonal Characteristics of the Gravity Waves

The duration of PMCC events in the frequency range from 10^{-4} to 10^{-3} Hz varies from 20 min to 3.3 h with an average duration of 1.6 h (Figure 4). In average, 11 events are observed per day. The duration of daily gravity wave activity varies from few hours to 24 h, the average duration being 14.6 h. The horizontal velocity varies from 20 to 40 m/s. The average wave amplitude is about 40 Pa after correction of the filter response, the maximum reaching 200 Pa for intense thunderstorms. This is in agreement with previous observations, reporting similar ranges of amplitudes [*Grachev et al*., 1995; *Koch and Siedlarz*, 1999].

The statistical study of data recorded during approximately 10 years reveals specific annual variations of the wave azimuth (Figure 5). Each year of the observation period, the azimuth of the gravity waves changes from south in February to east in May and north in August. The direction returns eastward in October and southward in December. The activity is weaker in January, and there is no activity coming from west of the station. Figure 6 (right) shows the south-north annual variation of the gravity wave azimuth, cumulated over the entire database. In order to identify the wave origin, this annual motion is compared to the cumulated motion of the thunderstorms shown in Figure 6 (left). This analysis uses WWLLN data [*Rodger et al*., 2009] recorded from 2005 to 2010 in a region centered on IS17 and extending from 10°S to 20°N and from 0°W to 10°W. This region corresponds to the thunderstorm azimuths as observed from the station. Comparison of both figures shows that gravity waves propagate northward when the thunderstorms are located to the south of the station (from January to May and from October to January) and southward when the thunderstorms are located to the north of the station (from May to October). This is also shown in the

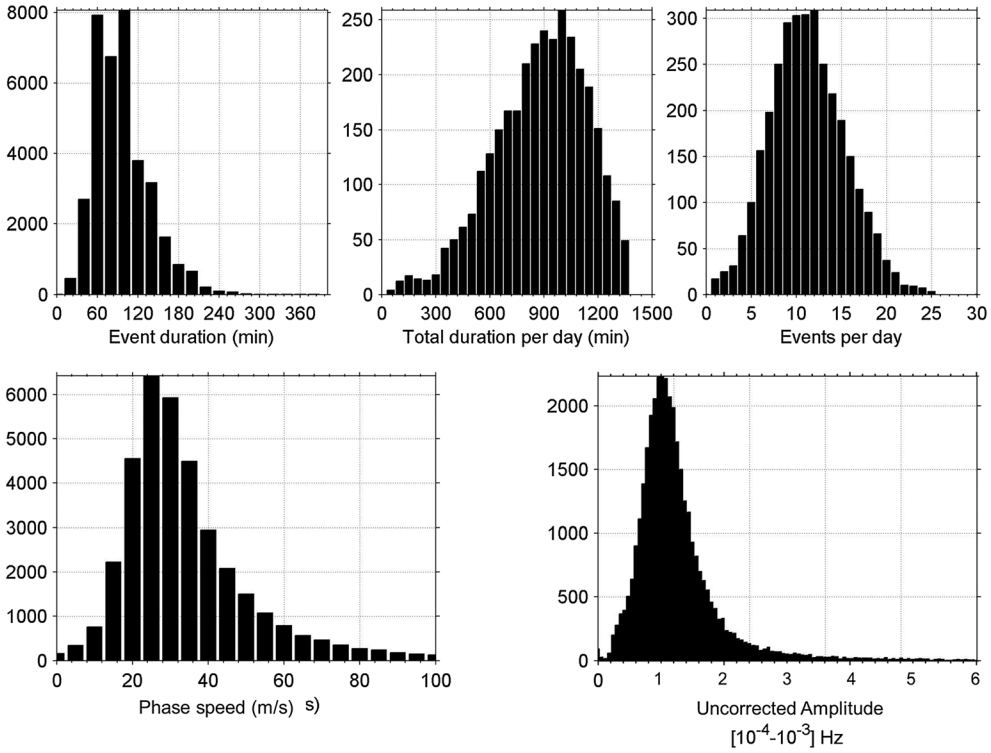

Figure 4. Characteristics of the gravity wave events observed at the IS17 station from April 2002 to December 2011. The analysis has been performed using the PMCC method in the frequency range from 10^{-4} to 10^{-3} Hz. The average horizontal phase velocity is 37 m/s, the average event duration is 1.6 h (96 min), the duration of the gravity wave activity varies from few hours to 24 h, and the average duration being 14.6 h (880 min). The average wave amplitude exceeds 0.5 Pa which corresponds to more than 100 about 40 Pa after correction of the sensor's frequency response.

different satellite lightning maps of several representative months of the year (Figure 7). These maps present the location of the lightning impacts measured by the Lightning Imaging Sensor (LIS) of the Tropical Rainfall Measuring Mission [*Christian et al.*, 2003]. Lightning flashes are observed to the south in February and to the north in July–August, like gravity wave observations.

The number of high-amplitude gravity wave events also shows seasonal variations including two activity periods in March–June and October–December and weaker activity in January (Figure 8). These annual variations are well correlated with the variations of the monthly keraunic level observed at the Lamto meteorological station located at about 40 km from IS17 and averaged over several years (1983 to 1992). The gravity wave activity periods correspond to the thunderstorm seasons observed near the station. The thunderstorm activity is very low in January similar to the gravity wave activity. This confirms the relation between gravity waves and thunderstorm activity.

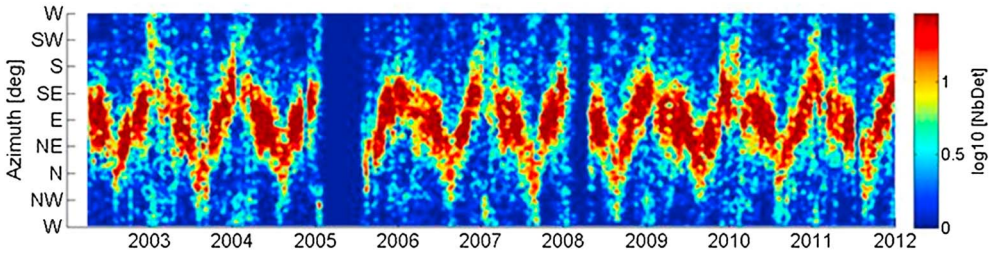

Figure 5. Ten years of gravity wave activity measured at IS17 infrasound station. The color scale indicates the logarithm of the number of detections.

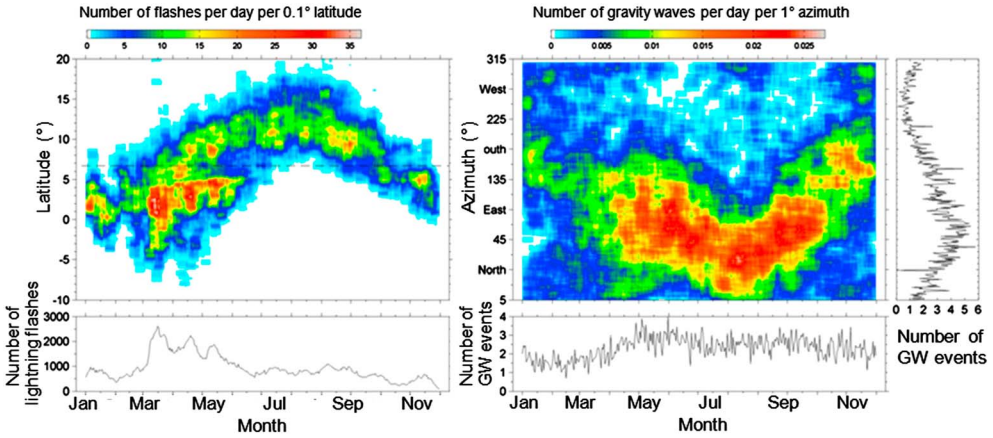

Figure 6. (right) Comparison between the cumulated gravity wave activity and (left) the cumulated lightning activity in the station longitude range, as observed from the station (azimuth represented by a dashed line). The station latitude is indicated by a dashed line. The color scale indicates the number of flashes per day per 0.1° latitude and the number of gravity waves per day per 1° azimuth, respectively. The gravity wave azimuth follows the lightning annual motion, north of the station in August, south in February.

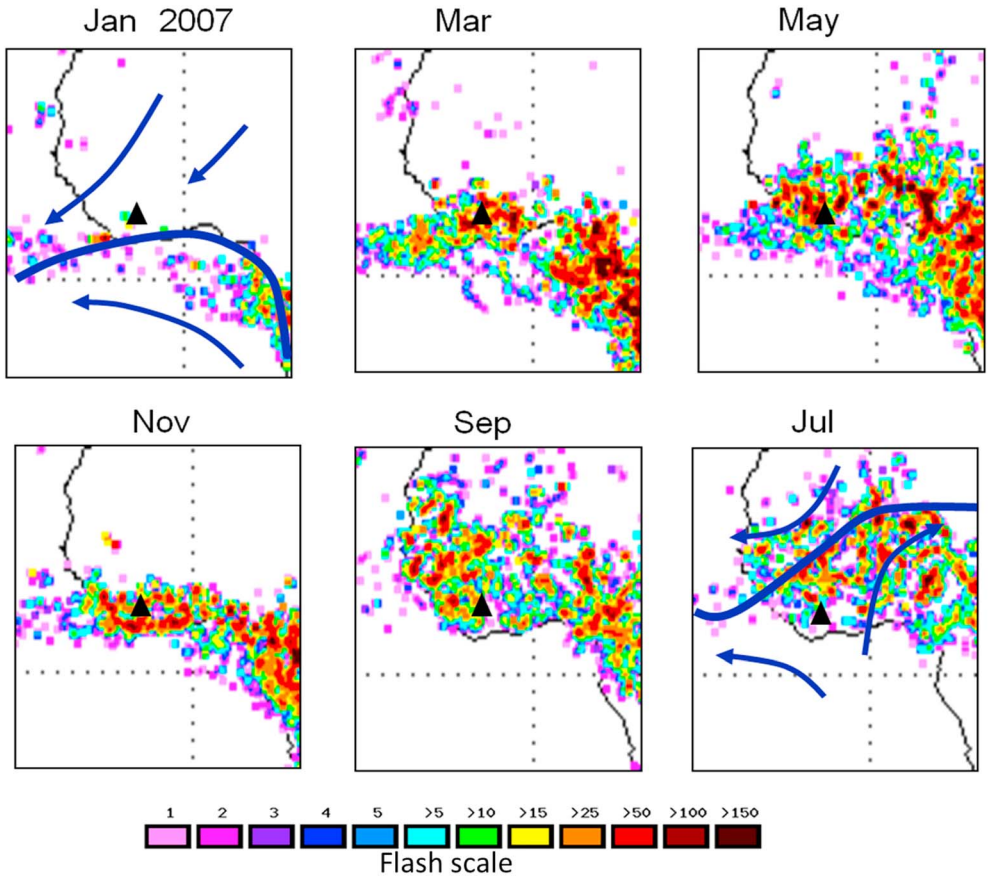

Figure 7. Variations of the location and number of lightning impacts during 1 year (2007) from satellite observations (LIS maps available on http://thunder.msfc.nasa.gov). The position of the Intertropical Convergence Zone of the surface winds in January and July is superimposed on the maps. IS17 is shown by a black triangle.

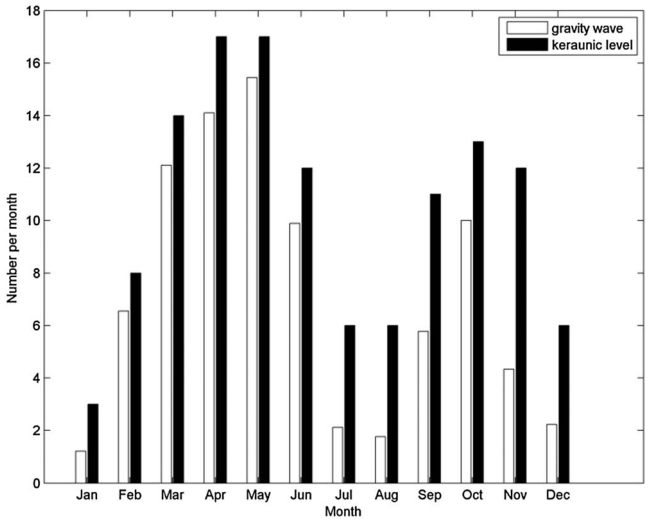

Figure 8. Comparison between the monthly number of strong gravity wave events measured at IS17 and the keraunic level at the Lamto station, showing good agreement between the annual gravity wave and thunderstorm activity.

3. Discussion

3.1. Thunderstorms at the Origin of the Observed Waves

The observations performed during the 10–11 April 2006 thunderstorm are in good agreement with previous observations [*Grachev et al*., 1995, 1997]. The characteristics of the observed pressure wave are similar in terms of amplitude fluctuations. The waveform consists in a first pressure decrease followed by a large pressure oscillations related to the different convection cells passing over the station. The azimuth corresponds to the arrival direction of the general thunderstorm motion. These results are also similar to other observations described by *Blanc et al*. [2010] for a large thunderstorm in Europe.

During the second part of the thunderstorm, the satellite maps show a more complex cloud system, and different gravity wave directions indicate the direction of several convection cells simultaneously active. The gravity waves disappear when the cloud moves away. The change of 180° in the wave direction of propagation, as previously observed by *Grachev et al*. [1995] when the convection system passes above the observation site, is only observed in the acoustic frequency range. Such infrasound signals are associated to the low-frequency part of the thunder [*Farges*, 2008; *Farges and Blanc*, 2010]. Their origin could be electrostatic field producing a reduction of atmospheric pressure inside the charged region of the cloud which is canceled when a lightning discharge occurs [*Few*, 1986]. The observed lightning azimuth differs from the gravity wave azimuth whose origin is convection. Comparisons between the waves and the cloud temperature show that the origin of the observed waves is related to deep convection. Wave activity is strong when the cloud temperature is low. The observed wave system reflects the structure of the different convective cells and represents the gravity wave formation inside the convection cells.

The correspondence between the lightning seasonal motion north and south of the station and the gravity waves motion shows the strong relation between gravity waves and thunderstorms. This motion is also the motion of the Intertropical Convergence Zone (ITCZ), formed by the easterly surface winds converging from both hemispheres in the equatorial region under the seasonal effect of solar radiation. West Africa ITCZ is the zone of convergence of southwesterly monsoon flow and the dry and hot northeasterly winds, known as "Harmattan." The interface between the two air masses is closely linked to pressure gradients across West Africa [e.g., *Buckle*, 1996]. The ITCZ motion differs from the rain belt motion [*Nicholson*, 2009] and then from lightning general motion. *Collier and Hughes* [2011] showed that the tropical lightning motion in this part of Africa is located south of the actual ITCZ position, due to the presence of Gulf of Guinea and Congo basin leading to thundercloud formation within the monsoon flow. In the present observations, the seasonal oscillation represents the motion of the deep convection related to convective thunderstorm and is then mostly related to the rain belt motion.

The second possible origin of gravity waves could be topographic [*Fritts and Alexander*, 2003]. The observed phase velocities are, however, low for topographic forcing. Also, surface winds are generally very low in this region. A study of 20 years of meteorological data in low-latitude regions showed that the winds in Ivory Coast are weak (generally lower than 3 m/s in July and even weaker in January) [*Nicholson and Grist*, 2003]. Such winds are much weaker than winds generally involved in the processes of mountain waves, which generally exceed 10 m/s [*Doyle et al*., 2005]. Moreover, there are no mountains around the station: IS17 is located about 100 km north of the Atlantic Ocean, which discards the possibility of generating mountain waves in this area. We conclude that the origin of the observed waves is mainly related to atmospheric convection in thunderstorms.

3.2. Conclusion and Perspectives

We have presented 10 years of observations by the IMS infrasound stations of gravity waves in tropical West Africa. The gravity wave activity is very strong during all the year with a maximum in April and October. We have demonstrated that this activity is produced by deep convection inside thunderstorm structures which dominate other possible sources of wave activity. Wave monitoring by infrasound stations in these regions can then determine the rain belt motion. Such measurements are also important for understanding the spectrum at low altitudes closer to wave sources.

A deeper analysis of such data set could provide a more precise description of changes at smaller scales of time, originating from other more complex processes. The precise climatology of these waves in equatorial regions, which are very active, and their interaction with the upper atmosphere need to be determined to improve weather and climate modeling. This is the objective of the ongoing European FP7 ARISE project.

Acknowledgments

We would like to thank the Director and the team of the Station Géophysique de Lamto in Ivory Coast for the very good and dedicated work they are doing in maintaining their infrasound network and in making the data available. The results obtained in this article would not have been possible without their involvement. We also thank P. Herry for the time he spent in data processing and Sergey Kulichkov and Sergey Kshevetskii for stimulating discussions, P. Husson, Meteo-France, for providing the Meteosat data, and the Worldwide Lightning Location Network (http://wwlln.net), a collaboration among over 50 universities and institutions, for providing the lightning location data used in this paper. The LIS/OTD climatology maps were obtained from the NASA's Global Hydrology and Climate Center (http://thunder.msfc.nasa.gov/). This work was performed in the frame of the ARISE project (www.arise-project.eu) 284387, funded by the European Union under the Seventh Framework Programme. The authors also would like to thank the reviewers for relevant comments.

References

Alexander, M. J., P. T. May, and J. H. Beres (2004), Gravity waves generated by convection in the Darwin area during the Darwin Area Wave Experiment, *J. Geophys. Res.*, *109*, D20S04, doi:10.1029/2004JD004729.

Assink, J. D., R. Waxler, and D. Drob (2012), On the sensitivity of infrasonic traveltimes in the equatorial region to the atmospheric tides, *J. Geophys. Res.*, *117*, D01110, doi:10.1029/2011JD016107.

Baldwin, M. P., D. W. J. Thompson, E. F. Shuckburgh, W. A. Norton, and N. P. Gillet (2003), Weather from the stratosphere?, *Science*, *301*, 317–319.

Blanc, E., A. Le Pichon, L. Ceranna, T. Farges, J. Marty, and P. Herry (2010), Global scale monitoring of acoustic and gravity waves for the study of the atmospheric dynamics, in "Infrasound monitoring for atmospheric studies" Springer editions.

Brachet, N., D. Brown, R. Le Bras, P. Mialle, and J. Coyne (2010), Monitoring the Earth's atmosphere with the global IMS infrasound network, in "Infrasound monitoring for atmospheric studies" Springer editions.

Buckle, C. (1996), *Weather and Climate in Africa*, 320 pp. Longman. Ltd, Harlow, U. K.

Campus, P., and D. R. Christie (2010), Worldwide observations of infrasonic waves, in "Infrasound monitoring for atmospheric studies" Springer editions.

Cansi, Y. (1995), An automatic seismic event processing for detection and location: The PMCC method, *Geophys. Res. Lett.*, *22*, 1021–1024, doi:10.1029/95GL00468.

Charlton, A. J., A. O'Neill, W. A. Lahoz, and C. Massacand (2004), Sensitivity of tropospheric forecasts to stratospheric initial conditions, *Q. J. R. Meteorol. Soc.*, *130*, 1771–1792, doi:10.1256/qj.03.167.

Christian, H. J., et al. (2003), Global frequency and distribution of lightning as observed from space by the Optical Transient Detector, *J. Geophys. Res.*, *108*(D1), 4005, doi:10.1029/2002JD002347.

Christie, D. R., and P. Campus (2010), The IMS infrasound network: Design and establishment of infrasound stations, in "Infrasound monitoring for atmospheric studies" Springer editions.

Collier, A. B., and A. R. W. Hughes (2011), Lightning and the African ITCZ, *J. Atmos. Sol. Terr. Phys.*, *73*, 2392–2398.

Costantino, L., and P. Heinrich (2013), Tropical deep convection and density current signature in surface pressure: Comparison between WRF model simulations and infrasound measurements, *Atmos. Chem. Phys. Discuss.*, *13*, 15,993–16,046.

Curry, M. J., and R. C. Murty (1974), Thunderstorm-generated gravity waves, *J. Atmos. Sci.*, *31*, 1402–1408.

Danilov, S. D., and A. I. Svertilov (1991), Internal gravity waves generated by a passage of thunderstorm, *Izv. Atmos. Oceanic Phys.*, *27*(3), 234–242.

Doyle, J. D., M. A. Shapiro, Q. Jiang, and D. L. Barlels (2005), Large-amplitude mountain wave breaking over Greenland, *J. Atmos. Sci.*, *62*, 3106–3126.

Farges, T. (2008), Infrasound from lightning and sprites, in *Lightning: Principles, Instruments and Application*, edited by H. D. Betz, U. Schumann, and P. Laroche, pp. 417–432, Springer, Dordrecht.

Farges, T., and E. Blanc (2010), Characteristics of infrasound from lightning and sprites near thunderstorm areas, *J. Geophys. Res.*, *115*, A00E31, doi:10.1029/2009JA014700.

Farges, T., E. Blanc, A. Le Pichon, T. Neubert, and T. Allin (2005), Identification of infrasound produced by sprites during the Sprite2003 campaign, *Geophys. Res. Lett.*, *32*, L01813, doi:10.1029/2004GL021212.

Few, A. A. (1986), Acoustic radiations from lightning, in *The Earth's Electrical Environment*, pp. 46–60, National Academy Press, Washington, D. C.

Fritts, D. C., and M. J. Alexander (2003), Gravity wave dynamics and effects in the middle atmosphere, *Rev. Geophys.*, *41*(1), 1003, doi:10.1029/2001RG000106.

Goerke, V. H., and M. W. Woodward (1966), Infrasonic observation of severe weather system, *Mon. Weather Rev.*, *94*(6), 395–398.

Gratchev, A. I., S. N. Kulichkov, and A. K. Matveyev (1988), Quasiperiodic atmospheric pressure fluctuations with periods from 20 to 180 min, *Izv. Atmos. Oceanic Phys.*, *24*(2), 111–114.

Grachev, A. I., S. D. Danilov, S. N. Kulichkov, and A. I. Svertilov (1995), Main characteristics of internal gravity waves from convective storms in the lower troposphere, *Izv. Atmos. Oceanic Phys.*, *30*(6), 725–733.

Grachev, A. I., S. N. Kulichkov, and A. I. Otrezov (1997), Spectral properties of internal gravity waves from thunderstorms, *Izv. Atmos. Oceanic Phys.*, *33*(5), 583–591.

Hauchecorne, A., J. L. Bertaux, F. Dalaudier, J. M. Russell, M. G. Mlynczak, E. Kyrölä, and D. Fussen (2007), Large increase of NO2 in the north polar mesosphere in January–February 2004: Evidence of a dynamical origin from GOMOS/ENVISAT and SABER/TIMED data, *Geophys. Res. Lett.*, *34*, L03810, doi:10.1029/2006GL027628.

Holton, J. R., P. H. Haynes, M. E. McIntyre, A. R. Douglass, R. B. Rood, and L. Pfister (1995), Stratosphere-troposphere exchange, *Rev. Geophys.*, *33*(4), 403–439, doi:10.1029/95RG02097.

Koch, S. E., and L. M. Siedlarz (1999), Mesoscale gravity waves and their environment in the central United States during STORM-FEST, *Mon. Weather Rev.*, *127*, 2854–2879.

Kulichkov, S. N., and G. A. Bush (2001), Rapid variations in infrasonic signals at long distances from one-type explosions, *Izv. Atmos. Oceanic Phys.*, *37*(3), 306–313.

Lalande, J.-M., O. Sèbe, M. Landès, P. Blanc-Benon, R. S. Matoza, A. Le Pichon, and E. Blanc (2012), Infrasound data inversion for atmospheric sounding, *Geophys. J. Int.*, *190*, 687–701, doi:10.1111/j.1365-246X.2012.05518.x.

Le Pichon, A., and Y. Cansi (2003), PMCC for infrasound data processing, inframatics, n°2, 1–9, June 2003.

Le Pichon, A., E. Blanc, and D. Drob (2005), Probing high-altitude winds using infrasound, *J. Geophys. Res.*, *110*, D20104, doi:10.1029/2005JD006020.

Le Pichon, A., L. Ceranna, and J. Vergoz (2012), Incorporating numerical modeling into estimates of the detection capability of the IMS infrasound network, *J. Geophys. Res.*, *117*, D05121, doi:10.1029/2011JD016670.

Le Pichon, A., L. Ceranna, C. Pilger, P. Mialle, D. Brown, P. Herry, and N. Brachet (2013), The 2013 Russian fireball largest ever detected by CTBTO infrasound sensors, *Geophys. Res. Lett.*, *40*, 3732–3737, doi:10.1002/grl.50619.

Liszka, L. J. (2004), The possible infrasound generation by sprites, *J. Low Freq. Noise Vib. Active Contr.*, *23*, 85–93, doi:10.1260/0263092042869838.

Lott, F., and L. Guez (2013), A stochastic parameterization of the gravity waves due to convection and its impact on the equatorial stratosphere, *J. Geophys. Res. Atmos.*, *118*, 8897–8909, doi:10.1002/jgrd.50705.

Lyons, W. A., S. A. Cummer, M. A. Stanley, G. R. Huffines, K. C. Wiens, and T. E. Nelson (2008), Super cells and sprites BAMS, *Bull. Am. Meteorol. Soc.*, *89*, 1165–1174.

Matoza, R. S., M. Landès, A. Le Pichon, L. Ceranna, and D. Brown (2013), Coherent ambient infrasound recorded by the International Monitoring System, *Geophys. Res. Lett.*, *40*, 429–433, doi:10.1029/2012GL054329.

Marty, J. (2010), Ondes de gravité atmosphériques observées par un réseau 430 mondial de microbaromètres. 431 PhD thesis, Univ. Pierre et Marie Curie, Paris. [Available at http://hal.archives-ouvertes.fr/docs/00/74/07/00/PDF/marty.pdf.]

Marty, J., D. Ponceau, and F. Dalaudier (2010), Using the International Monitoring System infrasound network to study gravity waves, *Geophys. Res. Lett.*, *37*, L19802, doi:10.1029/2010GL044181.

Marty, J., F. Dalaudier, D. Ponceau, E. Blanc, and U. Munkhuu (2013), Surface pressure fluctuations produced by the total solar eclipse of 1 August 2008, *J. Atmos. Sci.*, *70*, 809–823, doi:10.1175/JAS-D-12-091.1.

Mitchell, D. M., L. J. Gray, J. Anstey, M. P. Baldwin, and A. Charlton-Perez (2013), The influence of stratospheric vortex displacements and splits on surface climate, *J. Clim.*, *26*(8), 2668–2682. ISSN 1520–0442, doi:10.1175/JCLI-D-12-00030.1.

Medeiros, A. F., M. J. Taylor, H. Takahashi, P. P. Batista, and D. Gobbi (2003), An investigation of gravity wave activity in the low-latitude upper mesosphere: Propagation direction and wind filtering, *J. Geophys. Res.*, *108*(D14), 4411, doi:10.1029/2002JD002593.

Nakamura, T., T. Aono, T. Tsuda, A. G. Admiranto, E. Achmad, and Suranto (2003), Mesospheric gravity waves over a tropical convective region observed by OH airglow imaging in Indonesia, *Geophys. Res. Lett.*, *30*(17), 1882, doi:10.1029/2003GL017619.

Neubert, T., et al. (2008), Recent results from studies of electric discharges in the mesosphere, *Surv. Geophys.*, doi:10.1007/s10712-008-9043-1.

Nicholson, S. E. (2009), A revised picture of the structure of the "monsoon" and land ITCZ over West Africa, *Clim. Dyn.*, *32*, 1155–1171, doi:10.1007/s00382-008-0514-3.

Nicholson, S. E., and J. P. Grist (2003), The seasonal evolution of the atmospheric circulation over West Africa and equatorial Africa, *J. Clim.*, *16*, 1013–1030.

Pautet, P.-D., M. J. Taylor, A. Z. Liu, and G. R. Swenson (2005), Climatology of short-period gravity waves observed over northern Australia during the Darwin Area Wave Experiment (DAWEX) and their dominant source regions, *J. Geophys. Res.*, *110*, D03S90, doi:10.1029/2004JD004954.

Pasko, V. P., U. S. Inan, and T. F. Bell (1997), Sprites as evidence of vertical gravity wave structures above mesoscale thunderstorms, *Geophys. Res. Lett.*, *24*(14), 1735–1738, doi:10.1029/97GL01607.

Ponceau, D., and L. Bosca (2010), Low noise broadband microbarometers, in "Infrasound monitoring for atmospheric studies" Springer editions.

Rodger, C. J., J. B. Brundell, R. H. Holzworth, and E. H. Lay (2009), Growing detection efficiency of the World Wide Lightning Location Network, Am. Inst. Phys. Conf. Proc., Coupling of thunderstorms and lightning discharges to near-Earth space: Proceedings of the Workshop, Corte (France), 23–27 June 2008, 1118, 15–20, doi:10.1063/1.3137706.

Rottger, J. (1977), Travelling disturbances in the equatorial ionosphere and their association with penetrative cumulus convection, *J. Atmos. Terr. Phys.*, *39*, 987–998.

São Sabbas, F. T., et al. (2010), Observations of prolific transient luminous event production above a mesoscale convective system in Argentina during the Sprite 2006 Campaign in Brazil, *J. Geophys. Res.*, *115*, A00E58, doi:10.1029/2009JA014857.

Sentman, D. D., and E. M. Wescott (1993), Observations of upper atmospheric optical flashes recorded from an aircraft, *Geophys. Res. Lett.*, *20*, 2857–2860, doi:10.1029/93GL02998.

Sentman, D. D., E. M. Wescott, R. H. Picard, J. R. Winick, H. C. Stenbaek-Nielsen, E. M. Dewan, D. R. Moudry, F. T. Sao Sabbas, M. J. Heavner, and J. Morrill (2003), Simultaneous observations of mesospheric gravity waves and sprites generated by a midwestern thunderstorm, *J. Atmos. Sol. Terr. Phys.*, *65*, 537–550.

Shaw, T. A., and T. G. Shepherd (2008), Raising the roof, *Nat. Geosci.*, *1*, 12.

Siefring, C. L., J. S. Morrill, D. D. Sentman, and M. J. Heavner (2010), Simultaneous near-infrared and visible observations of sprites and acoustic-gravity waves during the EXL98 campaign, *J. Geophys. Res.*, *115*, A00E57, doi:10.1029/2009JA014862.

Snively, J. B., and V. P. Pasko (2003), Breaking of thunderstorm-generated gravity waves as a source of short-period ducted waves at mesopause, *Geophys. Res. Lett.*, *30*(24), 2254, doi:10.1029/2003GL018436.

Vadas, S. L., D. C. Fritts, and M. J. Alexander (2003), Mechanism for the generation of secondary waves in wave breaking regions, *J. Atmos. Sci.*, *60*, 194–214.

Yue, J., S. L. Vadas, C.-Y. She, T. Nakamura, S. C. Reising, H.-L. Liu, P. Stamus, D. A. Krueger, W. Lyons, and T. Li (2009), Concentric gravity waves in the mesosphere generated by deep convective plumes in the lower atmosphere near Fort Collins, Colorado, *J. Geophys. Res.*, *114*, D06104, doi:10.1029/2008JD011244.